A 2-MHz 2-kW voltage-source inverter for low-temperature plasma generators: implementation of fast switching with a third-order resonant circuit

Hideaki Fujita
Okayama University

Hirofumi Akagi
Okayama University

A 2 MHz, 2 kW Voltage-Source Inverter for Low-Temperature Plasma Generators: Implementation of Fast Switching with a Third-Order Resonant Circuit

Hideaki Fujita, *Member, IEEE*, and Hirofumi Akagi, *Fellow, IEEE*

Abstract— **This paper presents a specially designed third-order resonant circuit intended to achieve fast switching operation for a voltage-source series-resonant inverter using four MOSFETs. The third-order resonant current superimposed on a sinusoidal load current helps to quickly charge or discharge the output capacitance of each MOSFET. This results not only in a reduction of the time required to turn the MOSFET on and off, but also in an improvement of the displacement factor of the inverter. Moreover, the third-order resonant circuit acts as a low-pass filter to eliminate the parasitic oscillation between line inductance and stray capacitance. The viability and effectiveness of the third-order resonant circuit is verified by a 2 MHz, 2 kW prototype inverter developed for a low-temperature plasma generator.**

I. Introduction

Low-temperature plasma has been applied to surface treatment processes for metallic parts, semiconductor materials, and so on. A high-frequency strong magnetic field produces low-temperature plasma from low-pressure gas and sustains it. A high-frequency power supply of 2–10 kW is required to generate the magnetic field in a frequency range of 2–13.56 MHz, which is too high for conventional semiconductor devices to perform their switching operations. A linear amplifier using BJTs or vacuum tubes has been applied to high-frequency power supplies for plasma generators at the expense of efficiency and size.

The emergence of fast switching devices such as power MOSFETs and SI devices has made it possible to implement high-frequency inverters for induction heating and discharge treating applications. However, a voltage-source inverter using MOSFETs has difficulty operating at more than 1 MHz. As each MOSFET is turned on, an electric charge stored in its inherent output capacitance may result not only in increased switching losses but also in an excessive surge voltage and spike current because the capacitance is shorted out. Thus, each MOSFET must be turned on after finishing the discharge. This may significantly degrade the displacement factor of the inverter in a high-frequency operation over 1 MHz because the discharge time is too long to be neglected.

This paper proposes a novel voltage-source series-resonant inverter equipped with a third-order resonant circuit which enables MOSFETs to perform fast-switching. A third-order resonant inductor is directly connected in series with the inverter output terminal, while a third-order resonant capacitor is connected in parallel with a main resonant circuit. The resulting third-order resonant current superimposed on a sinusoidal load current helps to achieve quick charge/discharge of the output capacitance of each MOSFET. This results not only in a reduction of the time required to turn the MOSFET on and off, but also in an improvement of the displacement factor of the inverter. Connection of the third-resonant current does not cause any increase in the peak current of the MOSFET, but causes a slight increase in the rms current. The third-order resonant circuit has an additional function of eliminating parasitic oscillation because it also acts as a low-pass filter for higher-order harmonic components contained in the square-wave output voltage of the inverter. Experimental results obtained from a 2 MHz, 2 kW voltage-source series-resonant inverter integrated into a low-temperature plasma generator, along with analytical results, verify the viability and effectiveness of the third-order resonant circuit introduced in this paper.

II. System Configuration

Fig.1 shows the system configuration of a 2 MHz 2 kW voltage-source inverter for a low-temperature plasma generator. The main circuit of the inverter is a single-phase H-bridge voltage-source inverter using four MOSFETs (2SK2057: TOSHIBA). The ratings and electrical characteristics of the MOSFETs are summarized in Table I. A loss-less snubber circuit connected to each MOSFET consists of only a 470 pF capacitor without any resistor or diode. The main series-resonant circuit is connected to the ac output of the inverter through a specially-designed third-order-resonant circuit and a step-down transformer of 10:1.

A third-order resonant inductor L_3 is directly connected in series with the inverter output terminals, while a third-order resonant capacitor C_3 is connected in parallel with the primary windings of the step-down transformer. The resulting third-order resonant current superimposed on a sinusoidal load current helps to achieve quick charge/discharge of the output capacitor of each MOSFET. This third-order resonant circuit additionally has the ability to eliminate parasitic resonance between the line inductance and the winding capacitance of the transformer because the third-order resonant circuit acts as a low-pass filter at any frequency higher than the third-order one.

The main series-resonant circuit consists of a water-

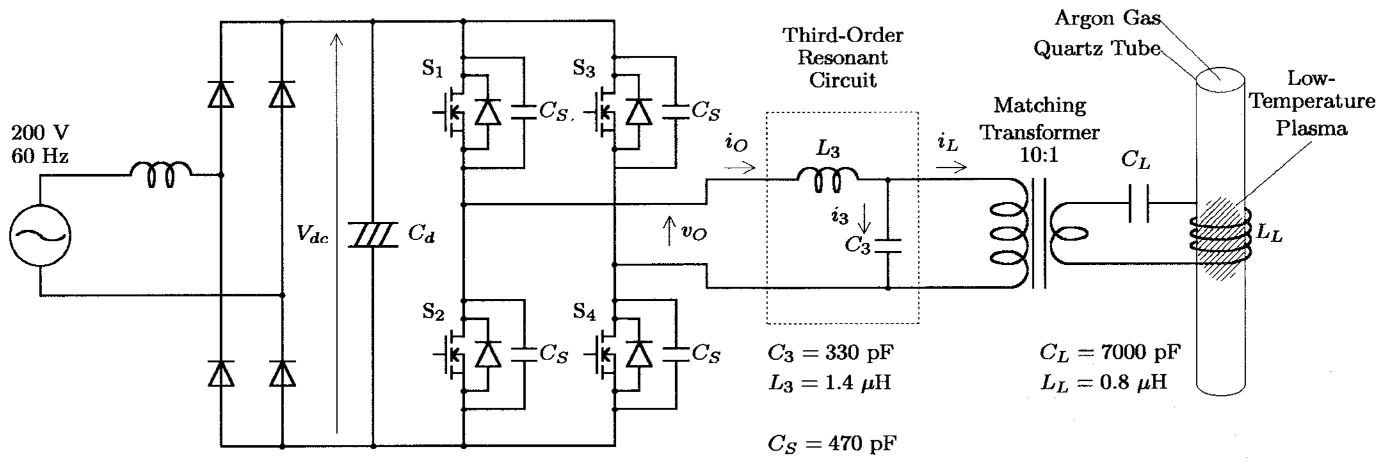

Fig. 1. System configuration.

TABLE I
RATINGS AND ELECTRICAL CHARACTERISTICS OF MOSFET (2SK2057).

		symbol	ratings	units
drain-to-source voltage		V_{DS}	500	V
gate-to-source voltage		V_{GS}	±30	V
drain current	DC	I_D	20	A
	pulse	I_{DP}	80	A
on-state resistance		$R_{DS(ON)}$	0.24	Ω
input capacitance		C_{iss}	3000	pF
output capacitance		C_{oss}	830	pF
switching times	rise time	t_r	25	ns
	turn-on delay	t_d(on)	60	ns
	fall time	t_f	55	ns
	turn-off delay	t_d(off)	280	ns

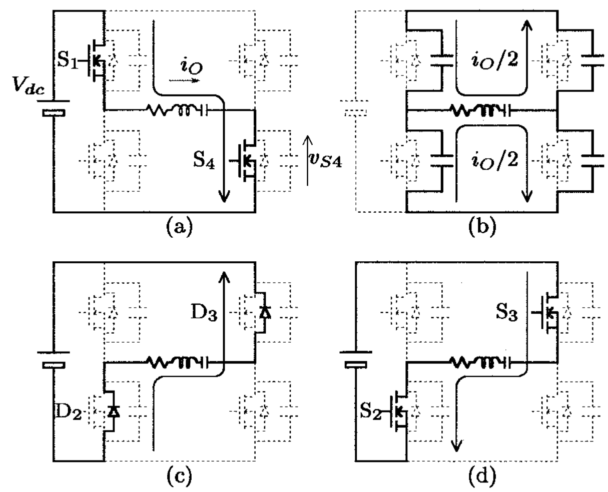

Fig. 2. Switching modes in the voltage-source inverter with a series resonant circuit. (a) Before commutation. (b) During commutation. (c) After commutation. (d) After load current direction change.

cooled seven-turn coil L_L and a high-frequency mica capacitor C_L. A quartz tube filled with argon gas, the diameter of which is 50 mm, is inserted into the resonant inductor L_L. A high-frequency magnetic field produced by the 2 MHz resonant current establishes and sustains low-temperature plasma in the quartz tube.

III. Switching Operation in Consideration of Output Capacitance of MOSFET

Fig.2 shows the switching modes in the voltage-source series-resonant inverter without the third-order resonant circuit, paying attention to the output capacitance of the MOSFET. Before commutation, MOSFETs S_1 and S_4 are conducting and the direction of the load resonant current is $i_O > 0$, as shown in Fig.2(a). Then the voltages across the output capacitors C_1 and C_4 are zero, while those across C_2 and C_3 are equal to the dc link voltage V_{dc}. Turning off S_1 and S_4 starts commutation, and the switching mode changes to Fig.2(b). During the commutation, the load resonant current discharges C_1 and C_4 while it charges C_2 and C_3. When the voltages across C_1 and C_4 reach V_{dc} and those across C_2 and C_3 become zero, free-wheeling diodes D_2 and D_3 start to conduct as shown in Fig.2(c). S_2 and S_3 are turned on with zero voltage after changing the direction of i_O, as shown in Fig.2(d), if the gate signals are provided during Fig.2(c). This means that time is required for the discharge of the output capacitance; in other words, the voltage-source inverter must be operated with a lagging displacement factor. If S_2 and S_3 are turned on before finishing the discharge, a large amount of surge voltage and spike current would appear in the drain-to-source voltage and the drain current due to the formation of a short circuit through S_2 and S_3. To avoid such a short circuit, S_2 and S_3 have to be turned on after the output capacitance is completely discharged. However, this may significantly decrease the displacement factor of the inverter in high-frequency operation over 1 MHz because the discharging time becomes too long to be neglected as the operating

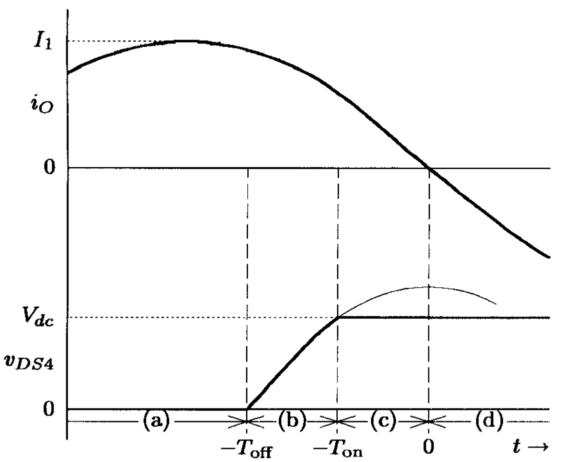

Fig. 3. Voltage and current waveforms.

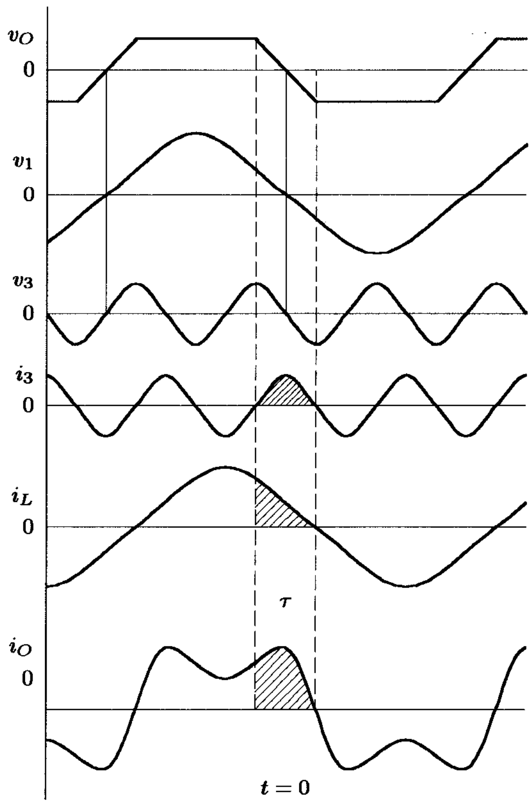

Fig. 4. Voltage and current waveforms in the third-order resonant circuit.

frequency increases.

Fig.3 shows the waveforms of the inverter output current i_O and the drain-to-source voltage v_{DS4}, taking into account the output capacitance of each MOSFET. Assuming that the direction of the inverter output current i_O changes at $t = 0$ and the rms value of i_O is I_1, i_O is represented as

$$i_O = -\sqrt{2} I_1 \sin \omega t. \tag{1}$$

S_1 and S_4 are turned off at $t = -T_{\rm off}$, and free-wheeling diodes D_2 and D_3 start to conduct at $t = -T_{\rm on}$. Since half of the load current, $i_O/2$, flows through the output capacitance of S_4 during the commutation (b), the drain-to-source voltage v_{DS4} is given by

$$v_{DS4} = \frac{1}{C_O} \int_{-T_{\rm off}}^{t} \frac{i_O}{2}\, dt = \frac{\cos \omega t - \cos \omega T_{\rm off}}{\sqrt{2} \omega C_O} I_1. \tag{2}$$

This implies that v_{DS4} has a sinusoidal wave shape having a peak value at $t = 0$ and that the peak value can be adjusted by the turn-off leading time $T_{\rm off}$. The drain-to-source voltage v_{DS4} has to reach V_{dc} before $t = 0$ to avoid the short circuit of the output capacitance. Thus, the minimum value of the turn-off leading time $T_{\rm off-min}$ is given by

$$T_{\rm off-min} = \frac{1}{\omega} \cos^{-1} \left\{ 1 - \frac{\sqrt{2} \omega C_S V_{dc}}{I_1} \right\}. \tag{3}$$

If S_1 and S_4 are turned off at $t = -T_{\rm off-min}$, and S_2 and S_3 are turned on at $t = 0$, all switches achieve zero-voltage switching without any short circuit. Moreover, no recovery current flows in the free-wheeling diodes because no diodes conduct during the commutation. The turn-off leading time $T_{\rm off}$, however, should be tuned for each leg due to the non-negligible difference in the output capacitance among the four MOSFETs. In practical applications, it is difficult to individually adjust the turn-off timing $T_{\rm off}$ for each MOSFET. To connect the loss-less snubber capacitor with each MOSFET results in adjustment-free operation although the displacement factor of the inverter output decreases according to the capacitance of the snubber capacitor.

IV. Fast Switching Operation Using Third-Order Resonant Circuit

The aim of the third-order resonant circuit proposed in this paper is to realize a fast discharge of the output capacitance by superimposing a third-order resonant current on the first-order (fundamental) load resonant current. The third-order resonant circuit allows the individual MOSFETs to perform fast switching without any surge voltage or spike current.

Fig.4 shows voltage and current waveforms when the third-order resonant circuit is connected, where v_1 and v_3 are the fundamental and third-order components included in the inverter output voltage v_O, respectively. Assuming that the inverter output voltage v_O is a square wave shape ignoring rise and fall times, the fundamental and third-order components v_1 and v_3 are given by the following equations:

$$v_1 = -\sqrt{2} \frac{2\sqrt{2} V_{dc}}{\pi} \sin \omega t \tag{4}$$

$$v_3 = -\sqrt{2} \frac{2\sqrt{2} V_{dc}}{3\pi} \sin 3\omega t. \tag{5}$$

Superimposing a third-order resonant current in phase with v_3 does not contribute to a fast charging or discharging of the output capacitance because v_3 is zero voltage at the center of the commutation period. A lagging current can quickly charge or discharge the output capacitance.

The resonant frequency of the third-order resonant circuit, ω_3 should be set to a specific frequency which is lower than three times as high as the operating frequency; that is, $\omega_3 < 3\omega$. The third-order resonant circuit acts as a reactive impedance for a third-order component included in the output square-wave voltage. Disregarding the resistance in the third-order resonant circuit represents the third-order resonant current i_3 as

$$i_3 = \sqrt{2}\frac{2\sqrt{2}V_{dc}}{3\pi(3\omega L_3 - 1/3\omega C_3)}\cos 3\omega t. \quad (6)$$

The third-order resonant current i_3 lags behind the third-order voltage v_3 by 90°; in other words, i_3 reaches its peak value at the center of the commutation period. The inverter output current, i_O has a quasi-trapezoidal wave shape shown in Fig.4 due to superimposing the third-order resonant current i_3. This results in fast charge or discharge of the output capacitance because i_O is larger than the load resonant current i_L during the commutation. The third-order resonant current i_3 makes it possible to increase the current only during the commutation without any increase of the peak value of i_O because the peak value of i_3 appears at the center of the commutation period. Therefore, the third-order resonant circuit i_3 should be tuned at a slightly lower frequency than three times as high as the operating frequency. Then the third-order resonant circuit acts as an inductive impedance which draws the third-order resonant current lagging by 90°.

V. Design Strategy of Third-Order Resonant Circuit

A. Design Strategy

The inverter output current i_O is a sum of the load resonant current i_L and the third-order resonant current i_3 given by

$$i_O = -\sqrt{2}I_1\sin(\omega t - \phi) + \sqrt{2}I_3\cos 3\omega t, \quad (7)$$

where I_1 and I_3 are the rms values of the load resonant current i_L and third-order resonant current i_3, and $\cos\phi$ is the displacement factor of the load resonant current.

The inverter output current i_O has to charge or discharge the output capacitance C_{oss} and snubber capacitor C_S in the upper and lower arms during the commutation period τ. This requirement is represented as

$$2Q_C = 2(C_{oss} + C_S)V_{dc} = \int_{-\tau/2}^{\tau/2} i_O\, dt, \quad (8)$$

where Q_C is the electric charge stored in C_{oss} and C_S. Accordingly, the amplitude of the third-resonant resonant current I_3 should be decided as

$$I_3 = \frac{3}{2}\frac{\sqrt{2}\omega Q_C + I_1\cos(\phi + \omega\tau/2) - I_1\cos(\phi - \omega\tau/2)}{\sin 3\omega\tau/2}. \quad (9)$$

In order to let the commutation finish at the instant that the load resonant current i_L is zero, the commutation period should be set as $\tau = 2\phi/\omega$. As a result, I_3 is obtained by

$$I_3 = \frac{3}{2}\frac{\sqrt{2}\omega Q_C + I_1\cos(\omega\tau) - I_1}{\sin 3\omega\tau/2} \quad (10)$$

By substituting (9) or (10) into (6), the impedance of the resonant circuit with respect to the third-order resonant frequency Z_3 is determined as

$$Z_3 = 3\omega L_3 - \frac{1}{3\omega C_3} = \frac{2\sqrt{2}V_{dc}}{3\pi I_3}. \quad (11)$$

Here, it is suitable to design the capacitance of C_3 as small as possible. Not only does the third-order resonant circuit draw the third-order resonant current, but it also acts as a capacitive impedance for the operating frequency. The third-order resonant capacitor C_3 should be designed to minimize the leading current.

B. Evaluation in Experimental System

In the experimental system shown in Fig.1, the resonant frequency of the load resonant circuit is 2.1 MHz, the rated resonant current is 9 A in rms value, and the dc link voltage of the inverter V_{dc}=200 V. Connecting the loss-less snubber capacitor of C_S=470 pF to each MOSFET, the electric charge stored in the output capacitance of the MOSFET and the snubber capacitor is given by

$$Q_C = (C_{oss} + C_S)V_{dc} = 0.42\ \mu\text{C}.$$

The commutation period should be made longer than the rise and fall times of the MOSFET used. A commutation period shorter than the rise or fall time would cause increased switching losses because the load resonant current flows through the MOSFETs even during the commutation period. Thus, the commutation period τ is set to the fall time in the experimental system, as $\tau = t_r = 55$ ns. From (10), the amplitude of the third-order resonant current is equal to 4.6 A in rms value. Thus, the resonant inductor and capacitor of the third-order resonant circuit, L_3 and C_3 have to be designed as $Z_3 = 16\ \Omega$. Assuming that $\phi/\omega = \tau/2$ in (10), the displacement factor of the inverter, $\cos\phi$ equals 94 %.

Fig.5 shows an equivalent circuit when both third-order resonant and load resonant circuits are connected, taking into account the turn ratio of the matching transformer. The equivalent reactor L_L' of the load resonant circuit is equal to $L_L' = nL_L$, and the equivalent capacitor C_L' equals $C_L' = C_L/n$, where n is the turn ratio of the matching transformer. The magnetizing inductance of the matching transformer can be ignored in Fig.5 because the magnetizing current is too small at the high-frequency operation of 2 MHz. The leakage inductance in the matching transformer is also negligible because it seems connected in series with L_L'.

A line inductance $\ell = 0.3\ \mu$H exists between the inverter bridge and the matching transformer, and the matching transformer has a parasitic capacitance $c = 240\ \mu$F in its primary windings. Taking into account the line inductance

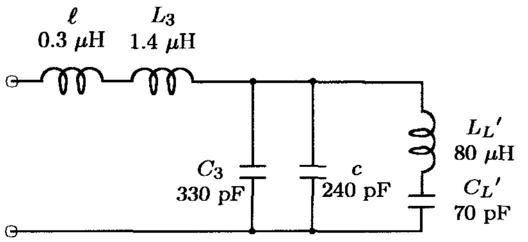

Fig. 5. Equivalent circuit of the third-order resonant circuit.

and the parasitic capacitance, the third-order resonant reactor L_3 is set to $L_3 = 1.4$ μH, and the third-order resonant capacitor $C_3 = 330$ pF. Thus, the resonant frequency equals 5.1 MHz. The impedance of the third-order resonant circuit is given by

$$3\omega L_3 - 1/(3\omega C_3) = 64 - 46 = 18\ \Omega.$$

Thus, the leading current drawn into the third-order resonant capacitor is

$$\frac{V1}{\omega C_3} = \frac{2\sqrt{2}}{\pi} \times 200/(2\pi \times 2 \times 10^6 \times 330 \times 10^{-12}) = 0.7\ \text{A},$$

which is less than 1/10 of the load resonant current. The voltage drop caused by the third-order resonant reactor L_3 is negligible because L_3 is only 2% of the load resonant reactor.

Amplitude variation in the case of operating frequency change is discussed below. Assume that the load resonant current is decreased by 1/2, according to frequency change. In this case, an increase of the operating frequency is only 1.7% because the load resonant circuit has a high quality factor of $Q = 50$ in the experimental system. The impedance of the third-order resonant circuit equals

$$3\omega L_3 \times 1.017 - 1/(3\omega C_3 \times 1.017) = 65 - 45 = 20\ \Omega.$$

This means that the variation in the third-order resonant current decreases by only 10 % even if such a large frequency change occurs, because the third-order resonant circuit is used in a frequency range, acting as a reactive impedance.

VI. Experimental Results

Fig.6 show experimental waveforms in the case of disconnecting the third-order resonant circuit. The inverter output current includes an oscillating current of 15 MHz because of parasitic resonance between the line inductance and the stray capacitance in the matching transformer. A surge voltage appears in the drain-to-source voltage because the MOSFETs are turned on before the discharge of the output capacitance. In Fig.6, both rise and fall times are about 80 ns, and the displacement factor is 88%.

Fig.7 shows experimental waveforms in the case of connecting the third-order resonant circuit. Since the third-order resonant current is superimposed on the load resonant current, the inverter output current i_O has a quasi-trapezoidal wave shape without any parasitic oscillation.

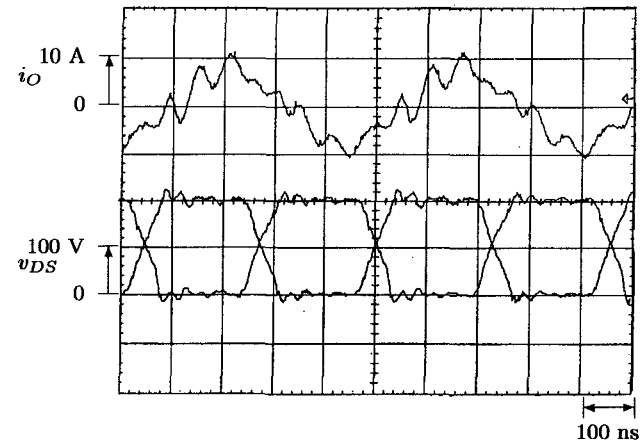

Fig. 6. Experimental waveforms in the case of disconnecting the third-order resonant circuit.

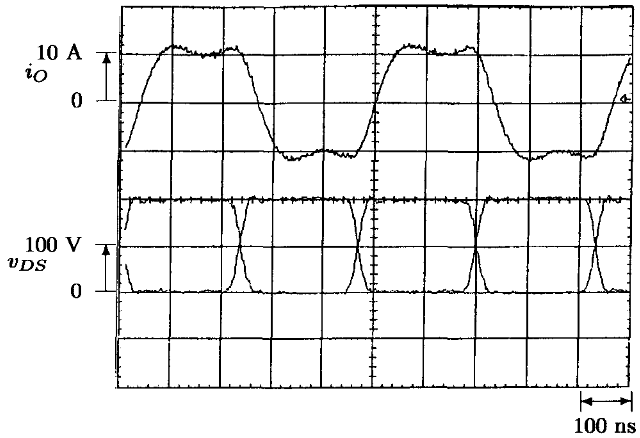

Fig. 7. Experimental waveforms in the case of connecting the third-order resonant circuit.

No surge voltage appears in the drain-to-source voltage because the third-order resonant current perfectly discharges the output capacitance before the corresponding MOSFETs are turned on. The rise and fall times are 40 ns in Fig.7, which equals half of those in Fig.6. This indicates that a high displacement factor of 97% is achieved by connecting the third resonant circuit. The dc input power of the inverter is 1800 W, and the high-frequency output power is 1690 W. Thus, the inverter efficiency is 94%, which confirms that the inverter performs a good switching operation even at frequencies as high as 2MHz.

Fig.8 shows experimental waveforms when no loss-less snubber capacitor is connected. The rise and fall times in Fig.8 equal 20 ns because the inverter output current i_O charges or discharges only the inherent output capacitance of each MOSFET. However, a surge voltage appears in the drain-to-source voltage v_{DS}. Note that the amount of the surge voltage in one arm is different from that in the other arm because of the differences in the output capacitance between the two MOSFETs and in the recovery time between the two free-wheeling diodes. Moreover, a small error of the turn-off time may produce a large surge

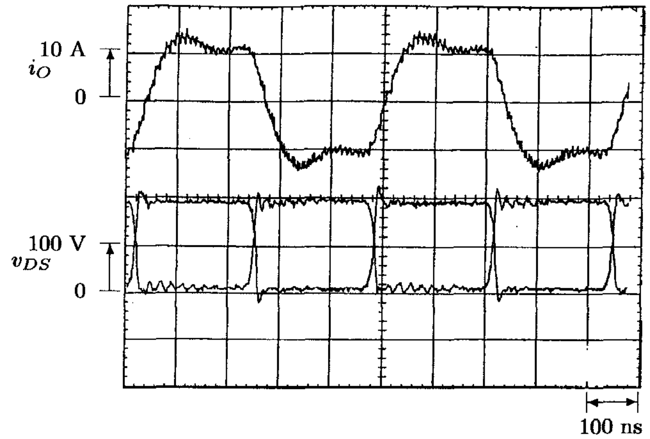

Fig. 8. Experimental waveforms in the case of disconnecting the loss-less snubber capacitor.

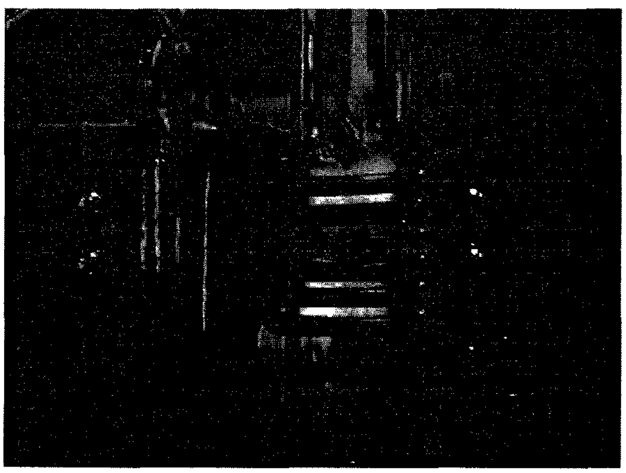

Fig. 9. Low-temperature plasma before flaming up (80 V, 10 A).

voltage, compared with the case of connecting the snubber circuit. Thus, an adjustment of the turn-off time for each arm is required to reduce such a surge voltage. It is, however, difficult to independently adjust the turn-off time in a practical application.

Figs.9 and 10 show states of low-temperature plasma generated by the inverter. Low-pressure argon gas is injected in the quartz tube and the output power of the inverter is adjusted by the dc link voltage in this experiment. After flaming up, the quality factor of the main resonant circuit decreases from 40 to 10 as shown in Fig.10 because of increased power consumption in the low-temperature plasma.

VII. Conclusion

A novel voltage-source series-resonant inverter with a third-order resonant circuit achieving a fast-switching operation has been proposed in this paper. The design strategy and practicability of the third-order resonant circuit have been discussed theoretically and experimentally. The third-order resonant current superimposed on a sinusoidal load current achieves quick charge/discharge of the output capacitance of each MOSFET.

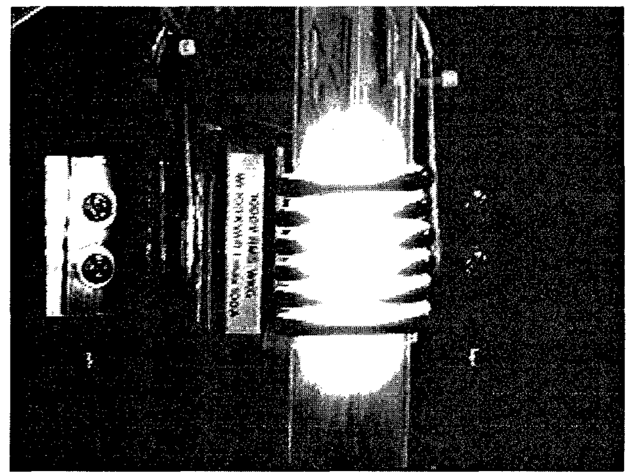

Fig. 10. Low-temperature plasma after flaming up (100 V, 5A).

Experimental results show a fast switching operation of 40 ns and a high displacement factor of 97% without any surge voltage or spike current. Moreover, a high efficiency of 94% is also obtained from the experiments, which verifies proper operation even at 2 MHz. The prototype system achieves the aims of generating a stable low-temperature plasma with high efficiency and of maintaining a small size.

Acknowledgment

The authors would like to thank Mr. Takeshi Okabe, and Mr. Kuniro Hirao, former graduate students in the department of Electrical Engineering at Okayama University, for their support in these experiments.

References

[1] Hans U. Eckert: "The Induction Arc: A State-of-the-art Review, " High Temperature Science, 6, pp.99–134, 1974

[2] W. E. Frank, C. F. Der, "Solid State RF Generators for Induction Heating Applications," IEEE/IAS Annual Meeting, pp.939–944, (1982)

[3] S. Bottari, L. Malesani, P. Tenti, "High Frequency 200 kHz Inverter for Induction Heating Applications," IEEE/PESC Rec., pp.308–316, (1985)

[4] H. Akagi, T. Sawae, A. Nabae, "130 kHz 7.5 kW Current-Source Inverters Using Static Induction Transistors for Induction Heating Applications," IEEE Trans. on Power Electronics, Vol. PE-3, No. 3, pp. 303–309, (1988)

[5] T. Yokoo, H. Itho, A. Sano: "High Frequency Inverter for Induction Heating Equipment by Using Static Induction Transistors," PCIM Proc., pp.101–108, (1988)

[6] P. P. Roy, S. R. Doradla, S. Deb: "Analysis of the Series Resonant Converter Using a Frequency Domain Model," IEEE/PESC Rec., pp.482–489, (1991)

[7] L. Grajales, J. A. Sabaté, K. R. Wang, W. A. Tabisz, F. C. Lee: "Design of a 10 kW, 500 kHz Phase-Shift Controlled Series-Resonant Inverter for Induction Heating," IEEE/IAS Annual Meeting, pp.843–849, (1993)

[8] H. Fujita, H. Akagi: "Pulse-Density-Modulated Power Control of a 4 kW, 450 kHz Voltage-Source Inverter for Induction Melting Applications," IEEE Trans. on IAS, Vol. 32, No. 2, pp.279–286, (1996)